N89-25157

MULTI-OBJECTIVE/LOADING OPTIMIZATION FOR ROTATING COMPOSITE FLEXBEAMS

BRIAN K. HAMILTON
JAMES R. PETERS

McDonnell Douglas Helicopter Company
Mesa, AZ

PRECEDING PAGE BLANK NOT FILMED

Introduction

With the evolution of advanced composites, the feasibility of designing bearingless rotor systems for high speed, demanding maneuver envelopes, and high aircraft gross weights has become a reality. These systems eliminate the need for hinges and heavily loaded bearings by incorporating a composite flexbeam structure which accommodates flapping, lead-lag, and feathering motions by bending and twisting while reacting full blade centrifugal force, Figure (1). The flight characteristics of a bearingless rotor system are largely dependent on hub design, and the principal element in this type of system is the composite flexbeam. As in any hub design, trade off studies must be performed in order to optimize performance, dynamics (stability), handling qualities, and stresses. However, since the flexbeam structure is the primary component which will determine the balance of these characteristics, its design and fabrication are not straightforward. Some of the considerations which must be addressed are as follows:

1. Flap-Lag-Torsion deformations will be accommodated through the flexbeam.
2. Effective flapping hinge offset has to be properly controlled for a balance between maneuverability and dynamic vibration.
3. Hub size must be kept at a minimum in order to reduce weight and hub drag.
4. Optimum tailoring of the pitchcase, snubber/damper and inplane flexbeam deformation must be obtained in order to maximize inplane damping.
5. The flexbeam must be able to endure peak loading from high g maneuvers as well as endurance flight loads.
6. Flexbeam design criteria are influenced by rotor shaft/mast/hub impedance characteristics.

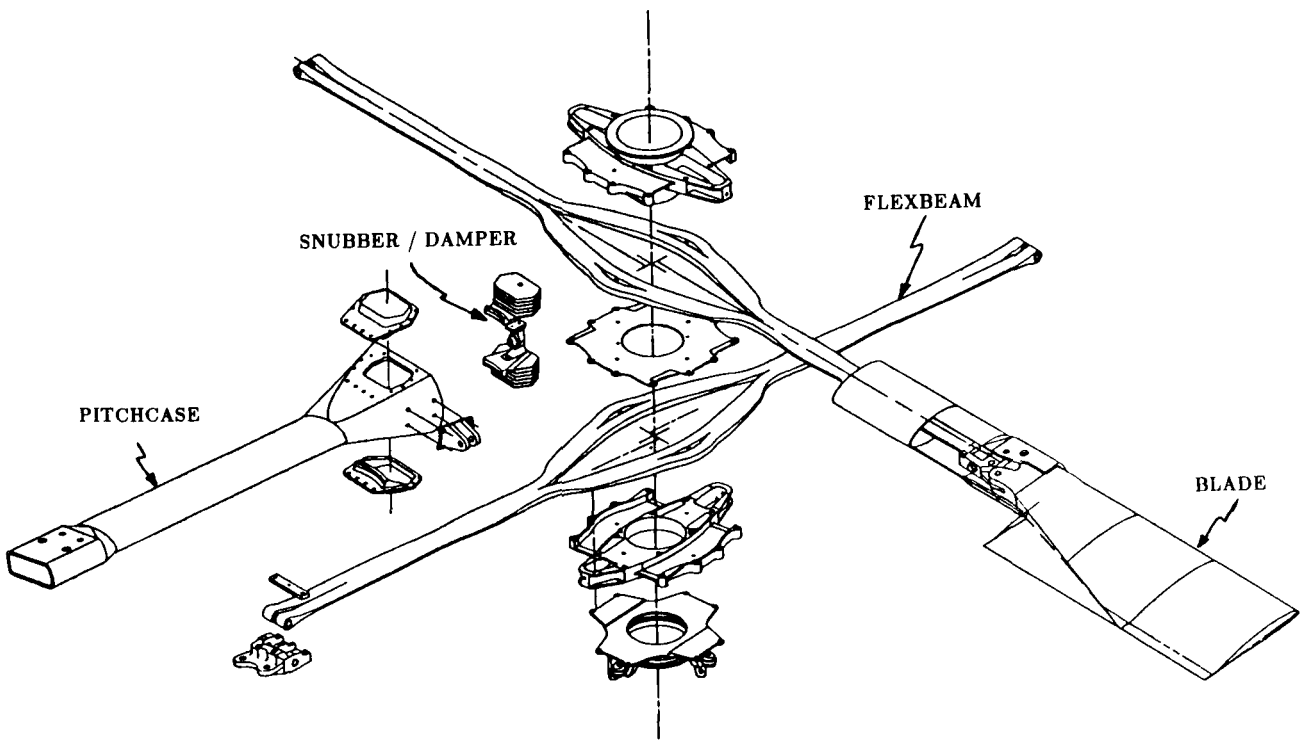

Figure (1)

Model Development

At McDonnell Douglas Helicopter Company, the previous considerations have been integrated into a mathmatical procedure for design and optimization of advanced composite bearingless rotor systems. Because of the highly coupled structural and damping requirements of the flexbeam, it was critical to include a representation of the pitchcase and snubber/damper, as well as the flexbeam, in the math model. Various alternatives can be proposed for formulation of such a problem:

1. choice of flexbeam cross section
2. choice of composite material type and configuration
3. choice of hub attachment configuration
4. choice of objective function and constraints for optimization routine
   (a) minimization of peak stresses due to flap, lag and torsion with a requirement on damper motion and hence rotor inplane damping
   (b) maximization of rotor damping with upper bound contraints on stresses

Flexbeam Cross Section

In an effort to simplify the beam design and fabrication, a comprehensive review of candidate cross sections was conducted under a company IRAD* program . Geometries studied ranged from rectangular, cruciform and multiple "H" closed sections to multiple element open sections and elastomericly connected rectangular cross sections.

Based on this review, a simple rectangular section was selected as the best overall configuration for the advanced flexbeam. In addition to the efficient load carrying capability, the relatively straightforward rectangular configuration offered advantages of simplified fabrication resulting in lower production costs, superior quality control, and simplified inspectability.

Composite Material Selection

The composite material selected for the advanced flexbeam was S-2 fiberglass impregnated with a 350 deg F cured "toughened resin" epoxy system. The resin system was selected based on the results of an extensive study of candidate systems conducted under other McDonnell Douglas Helicopter Company IRAD programs.

The S-2 fiberglass provides improved compressive stress margins and reduces long term enviromental degradation concerns associated with the previously selected Kevlar material.

---

*Internal Research and Development

Hub Attachment Configuration

Flexbeam design criteria are influenced by rotor shaft/ mast/hub impedance characteristics. A relatively soft rotor mast mount can significantly modify a flexbeam's effective flapping hinge offset and bending requirements. An inhouse analysis has indicated that a softer mount can result in an increased level of airframe vibration and the need for vibration suppression systems.

The Helicopter Advanced Rotor Program (HARP) flight test program demonstrated low vibration characteristics for the initial composite flexbeams using the McDonnell Douglas Helicopter Company rigid mast system with no active or passive vibration control equipment required. The advanced beam design approach was also based on the proven rigid mast configuration.

Objective Function and Constraints

Significant progress has been made both by industry and the goverment in the study of flexbeam design over the past ten years. McDonnell Douglas Helicopter Company has kept abreast of this work and has incorporated the lessons learned both by ourselves and other investigators into the present math model.

The primary goal in flexbeam sizing is to achieve the required rotor blade motions without exceeding the allowable stresses in the composite material. Simultaneous goals are to minimize flexbeam length, to achieve blade flap and lead-lag hinge offsets which provide suitable dynamics properties, and to obtain sufficient lead-lag motion at the snubber/damper for satisfactory dynamic response to cyclic loads. The criteria for blade motions include the maximum blade cyclic flap, lead-lag, and feathering motions seen in the flight envelope (the one hour condition), as well as endurance limit, static droop and start-up conditions.

Rotor blade flapping, lead-lag and feathering motions acting in combination with the blade and pitchcase centrifugal force cause flexbeam deformations. The flexbeam must be so designed as to allow these blade motions without exceeding the allowable stresses of the fiber composite of which it is constructed. Because blade motions have both steady and cyclic components, fatigue loads prevail and the fatigue strength of the composite material is critical for design. Therefore, the one hour and endurance limit flap, lead-lag, and torsional motions are applied to the flexbeam. The cyclic stresses which the one hour motions cause should not exceed the corresponding one hour fatigue allowables of the composite material. Similarly, cyclic stresses due to endurance limit loads should not exceed endurance limit fatigue allowables. In addition, criteria for the blade motions include static droop and start-up torque conditions. These goals, taken together, are used in sizing the flexbeam in lieu of a complete fatigue life analysis covering the full operating spectrum of the helicopter.

The objective function selected for the advanced beam was minimization of stresses due to a critical combination of flap, lead-lag and torsional deformation. In addition, a displacement constraint is imposed for adequate damper motion to satisfy the dynamic requirements.

Theoretical Background

The conventional finite element method is not applicable in the case of an elastic structure undergoing high angular motions. This is of interest because numerous structural configurations such as spinning helicopter blades, satellites, rotating flexbeams, shafts and linkages fall into this category. The analysis of these rotating structures differs from that of stationary structures due to the complexity of the accelerations which act throughout the system. In addition to the accelerations resulting from elastic structural deformations, contributions due to Coriolis and centripetal acceleration may be of significance. Also, the stiffness characteristics of the structure may be modified by the internal loads induced by the centrifugal forces. The finite element formulation given in this section includes all these effects in a uniform general formulation.

The variational principle useful for problems in dynamics is Hamilton's principle. The functional for this principle is the Lagrangian, L, defined as

$$L = T - U - V \tag{1}$$

where T is the kinetic energy, U is the strain energy, and V is the potential of the applied loads. The strain energy density may be expressed as

$$dU = \frac{1}{2}\varepsilon^T \sigma dV = \frac{1}{2}\varepsilon^T C \varepsilon dV \tag{2}$$

where C is the material elastic matrix. The potential of the applied loads, V, may be expressed as the sum of the potential of the body forces and surface tractions as

$$V = -\int_V (\bar{X} \cdot u) dV - \int_S (\bar{T} \cdot u) dS \tag{3}$$

where $\bar{X}$ is the body force vector, u is the displacement vector, and $\bar{T}$ is the vector of surface tractions. The second integral is over the surface of the body on which the surface tractions are prescribed.

The total kinetic energy density is defined as

$$dT = \frac{1}{2}\rho V^T V dV \tag{4}$$

where ρ is the density of the material and V is the absolute velocity of a particle in the element as given by

$$V = V_{RB} + \dot{u} + \tilde{\omega} u \tag{5}$$

Here, V_{RB} is the velocity of the particle due to frame motion, u is the vector of elastic deformations, and ω is the angular velocity of the element coordinate system. Substitution of equation (5) into (4) gives

$$dT = \frac{1}{2}\rho V_{RB}^T V_{RB} dV + \frac{1}{2}\rho \dot{u}^T \dot{u} dV$$
$$+\frac{1}{2}\rho(\dot{u}^T\tilde{\omega}u - u^T\tilde{\omega}\dot{u} - u^T\tilde{\omega}\tilde{\omega}u)dV$$
$$+\frac{1}{2}\rho(V_{RB}^T\dot{u} + \dot{u}^T V_{RB} + V_{RB}^T\tilde{\omega}u - u^T\tilde{\omega}V_{RB})dV \tag{6}$$

The first term in equation (6) is the kinetic energy due purely to frame translation. This term will be deleted since frame motion is assumed to be entirely prescribed. The second term represents the kinetic energy due to elastic deformations only. The third term is the energy due to frame rotation, and the fourth term gives the forces due to coupling between frame translation, elastic deformations and frame rotation.

Using equations (2), (3) and (6), the functional in equation (1) may be expressed in the following form:

$$L = \frac{1}{2}\int_V \rho\left(\dot{u}^T\dot{u} + \dot{u}^T\tilde{\omega}u - u^T\tilde{\omega}\dot{u} - u^T\tilde{\omega}\tilde{\omega}u\right)dV$$
$$-\frac{1}{2}\int_V \epsilon^T C\epsilon dV$$
$$+\frac{1}{2}\int_V \rho(V_{RB}^T\dot{u} + \dot{u}^T V_{RB} + V_{RB}^T\tilde{\omega}u - u^T\tilde{\omega}V_{RB})dV$$
$$+\int_V u^T\bar{X}dV + \int_S u^T\bar{T}dS \tag{7}$$

The statement of Hamilton's principle is as follows: Among all possible time histories of displacement configurations which satisfy compatibility and the constraints or kinematic boundary conditions and which also satisfy conditions at times t_1 and t_2, the history which is the actual solution makes the Lagrangian functional a minimum. This principle may be expressed mathematically as

$$\delta\int_{t_1}^{t_2} L dt = 0 \tag{8}$$

Application to the Finite Element Method

Most problems are too complex to use energy principles to obtain the exact solution directly. The usual technique is to guess, a priori, a trial family of solutions for the unknown quantity in order to construct a variational functional. We therefore choose an approximate pattern for the trial solution and apply the energy principles to the approximate functional to obtain the equations necessary to find the approximate solution. In the theory of the finite element method for structural analysis, once the proper variational principle has been selected for the given problem, we express the functional involved in terms of approximate assumed displacement functions which satisfy the geometric boundary conditions. We then minimize the approximate functional using equation (8) to obtain a set of governing equations.

General Displacement Models

The basic philosophy of the finite element method is piecewise approximation. That is, we approximate a solution to a complicated problem by subdividing the region of interest and representing the solution within each subdivision by a relatively simple function. In the displacement method of structural analysis, the structure or body is divided into finite elements. Then, simple functions are chosen to approximate the displacements within each element. These functions are called displacement models, displacement functions, displacement fields, or displacement patterns. A polynomial is the most common form of displacement model used for two principal reasons. First, it is easy to handle the mathematics of polynomials in formulating the desired equations for various elements and in performing digital computation. In particular, the use of polynomials permits us to differentiate and integrate with relative ease. Secondly, a polynomial of arbitrary order permits a recognizable approximation to the true solution; however, for practical purposes we are limited to one of finite order. By truncating an infinite polynomial at different orders, we clearly vary the degree of approximation.

An exact solution for the displacement $u(x)$ is then approximated by various degree polynomials of the general form

$$u(x) = \alpha_1 + \alpha_2 x + \alpha_3 x^2 + \cdots + \alpha_{n+1} x^n \tag{9}$$

The greater the number of terms included in the approximation, the more closely the exact solution is represented. In equation (9), the coefficients of the polynomial, the α's, are known as generalized coordinates or generalized displacement amplitudes. The number of terms retained in the polynomial determines the shape of the displacement model, whereas the magnitudes of the generalized coordinates govern the amplitude. These amplitudes are called generalized because they are not necessarily identified with the physical displacements of the element on a one-to-one basis; rather, they are linear combinations of some of the nodal displacements and perhaps of some of the derivatives of displacements at the nodes as well. The generalized coordinates represent the minimum number of parameters necessary to specify the polynomial amplitude.

Equation (9) can be expressed in vector form as

$$u(x) = \phi^T \alpha \tag{10}$$

where

$$\phi = \{1 x x^2 x^3 \cdots x^n\}^T,$$

and

$$\alpha = \{\alpha_1 \alpha_2 \alpha_3 \cdots \alpha_{n+1}\}^T.$$

The degrees of freedom can thus be related to the generalized coordinate system by employing the displacement model. We can evaluate the generalized displacements at the nodes by substituting the nodal coordinates into the model. For example, using a model of the form given by equation (10), we may write, for a single node point

$$u(x) = \phi \alpha \tag{11}$$

where u is the vector of degrees of freedom for a single node; or, for the entire element,

$$x = \begin{Bmatrix} u(node1) \\ u(node2) \\ \cdots \\ u(nodeN_n) \end{Bmatrix} = \begin{bmatrix} \phi(node1) \\ \phi(node2) \\ \cdots \\ \phi(nodeN_n) \end{bmatrix} \alpha = A\alpha \tag{12}$$

where N_n is the total number of nodes for the element being considered, x is the vector of nodal degrees of freedom, and the notation in parentheses indicates that the dependent variables are assigned their values at the particular node. We may invert equation (12) to get

$$\alpha = A^{-1}x \tag{13}$$

where A^{-1} is a displacement transformation matrix. Note that A is a square matrix, hence, the total number of generalized coordinates equals the total number of joint and internal degrees of freedom. Equation (13) may then be used to eliminate the generalized coordinates to obtain

$$u = \phi A^{-1}x = Nx \tag{14}$$

which expresses the displacements u at any point within the element in terms of the displacements of the nodes x.

Since the derivations of the element matrices are performed in the α coordinate system, we further develop the necessary relationships in terms of the generalized α coordinates rather than the physical x coordinates.

The strains are expressed in terms of some combination of the derivatives of the displacements u. Since the generalized coordinates α are not functions of the spatial coordinates, these derivatives must be performed in terms of the matrix ϕ. If ε is the vector of the relevant strain components at an arbitrary point within the finite element, we use the strain-displacement equations and the displacement model to write

$$\varepsilon = B_\alpha \alpha \tag{15}$$

It is important to note that for geometrically nonlinear problems ε and B_α are functions of the independent space coordinates as well as functions of the generalized coordinates. Decomposing these quantities into linear and nonlinear parts, we have

$$\varepsilon = \varepsilon_l + \varepsilon_{nl} \tag{16}$$

and therefore,

$$B_\alpha = B_{\alpha_l} + B_{\alpha_{nl}} \tag{17}$$

If σ is the vector of stresses corresponding to the strains ϵ, we may use an appropriate matrix form of the stress strain equations and equation (15) to write the element stresses as

$$\sigma = CB_\alpha \alpha \tag{18}$$

where C is the matrix of material constants given by equation (3).

Variational Formulation of Element Matrices

As discussed above, the method used here for calculating the element matrices and load vectors is the application of Hamilton's principle. Therefore, we develop the Lagrangian given in equation (7) in terms of the α generalized coordinates and apply equation (8) to obtain the element equations in terms of the generalized coordinates and shape functions.

In order to formulate the Lagrangian in terms of the generalized coordinates, we insert equations (11), (15) and (18) into equation (7) to obtain

$$\begin{aligned} L = & \frac{1}{2}\int_V \alpha^T B_\alpha^T C B_\alpha \alpha dV \\ & -\frac{1}{2}\int_V \rho\left(\dot{\alpha}^T\phi^T\phi\dot{\alpha} + \dot{\alpha}^T B_2\alpha - \alpha^T B_2\dot{\alpha} - \alpha^T B_1\alpha\right)dV \\ & -\frac{1}{2}\int_V \rho\left(V_{RB}^T\phi\dot{\alpha} + \dot{\alpha}^T\phi^T V_{RB} + V_{RB}^T\tilde{\omega}\phi\alpha - \alpha^T\phi^T\tilde{\omega}V_{RB}\right)dV \\ & -\int_V \alpha^T\phi^T\bar{X}dV - \int_S \alpha^T\phi^T\bar{T}dS \end{aligned} \tag{19}$$

where

$$B_1 = \phi^T\tilde{\omega}\tilde{\omega}\phi \tag{20}$$

and

$$B_2 = \phi^T\tilde{\omega}\phi \tag{21}$$

Applying the variational principle given by equation (8), we obtain

$$\begin{aligned} & \int_{t_1}^{t_2}\left(\delta\alpha^T\int_V (B_\alpha^T C B_\alpha + B_\sigma)dV\,\alpha - \delta\dot{\alpha}^T\int_V \rho\phi^T\phi dV\,\dot{\alpha}\right)dt \\ & + \int_{t_1}^{t_2}\left(-\delta\dot{\alpha}^T\int_V \rho B_2 dV\,\alpha + \delta\alpha^T\int_V \rho B_2 dV\,\dot{\alpha}\right)dt \\ & + \int_{t_1}^{t_2}\left(\delta\alpha^T\int_V \rho B_1 dV\,\alpha\right)dt \\ & - \int_{t_1}^{t_2}\left(\delta\dot{\alpha}^T\int_V \rho\phi^T V_{RB}dV - \delta\alpha^T\int_V \rho\phi^T\tilde{\omega}V_{RB}dV\right)dt \\ & - \int_{t_1}^{t_2}\left(\delta\alpha^T\int_V \phi^T\bar{X}dV + \delta\alpha^T\int_S \phi^T\bar{T}dS\right)dt = 0 \end{aligned} \tag{22}$$

where the matrix B_σ arises from the variation of the nonlinear part of the matrix B_α which is a function of the generalized coordinates α. The i^{th} row of the matrix B_σ is given by

$$B_{\sigma_i} = \alpha^T B_{\alpha_l}^T C \frac{\partial B_{\alpha nl_i}}{\partial \alpha_i} \tag{23}$$

for $i = 1, 2, \cdots, 12$. Integration of the terms in equation(22) by parts with respect to time gives

$$\begin{aligned}
&\int_{t_1}^{t_2} \delta\alpha^T \left(\int_V \rho\phi^T \phi dV \ddot{\alpha} + \int_V 2\rho B_2 dV \dot{\alpha} \right) dt \\
&+ \int_{t_1}^{t_2} \delta\alpha^T \left(\int_V (B_\alpha^T C B_\alpha + B_\sigma + \rho\dot{B}_2 + \rho B_1) dV \alpha \right) dt \\
&+ \int_{t_1}^{t_2} \delta\alpha^T \left(\int_V (\rho\phi^T \dot{V}_{RB} + \rho\phi^T \tilde{\omega} V_{RB}) dV \right) dt \\
&- \int_{t_1}^{t_2} \delta\alpha^T \left(\int_V \phi^T \bar{X} dV - \int_S \phi^T \bar{T} dS \right) dt = 0
\end{aligned} \tag{24}$$

Since the variations of the generalized displacements, $\delta\alpha$, are arbitrary, the sum of the expressions in parentheses must vanish. Therefore we obtain the equations of motion for the element as

$$M^\alpha \ddot{\alpha} + C^\alpha \dot{\alpha} + K^\alpha \alpha = F^\alpha \tag{25}$$

where M^α is the consistent mass matrix defined by

$$M^\alpha = \int_V \rho\phi^T \phi dV \tag{26}$$

C^α is the damping matrix due to frame motion as given by

$$C^\alpha = 2 \int_V \rho B_2 dV \tag{27}$$

and K^α is the element stiffness matrix in terms of α coordinates as given by

$$K^\alpha = \int_V (B_\alpha^T C B_\alpha + B_\sigma) dV + \int_V \rho(B_1 + \dot{B}_2) dV \tag{28}$$

The first integral in the above equation is the stiffness due to strain energy and will be referred to as K_u^α. The second integral is the stiffness due to frame motion to be referred to as K_m^α. Recall from equation (17) that B_α is comprised of linear and nonlinear parts. Then the stiffness due to strain energy, K_u^α, may be decomposed into linear and nonlinear parts to give

$$K_{u_l}^\alpha = \int_V B_{\alpha_l}^T C B_{\alpha_l} dV \tag{29}$$

$$K^{\alpha}_{u_{nl}} = \int_V B^T_{\alpha_l} C B_{\alpha_{nl}} dV + \int_V B^T_{\alpha_{nl}} C B_{\alpha_l} dV$$
$$+ \int_V B_{\alpha_{nl}}{}^T C B_{\alpha_{nl}} dV + \int_V B_\sigma dV \tag{30}$$

The stiffness matrix resulting from the first three terms in equation (30) is known as the *large displacement* matrix. The stiffness matrix arising from B_σ is dependent on the stress level and is known as the *initial stress* matrix, Ref. (1).

Finally, the load vector, F^α, is defined by

$$F^\alpha = \int_V \phi^T \bar{X} dV + \int_S \phi^T \bar{T} dS$$
$$- \int_V (\rho \phi^T \dot{V}_{RB} + \rho \phi^T \tilde{\omega} V_{RB}) dV \tag{31}$$

Displacement Models for a Beam Element

Having formulated the expressions for the element matrices and loads in terms of the general shape functions, the next step is to choose the displacement models that will approximate the solution for the problem at hand. A flexbeam is a cantilever beam under tension. For a beam element, axial, lateral and torsional deformations are of interest. To approximate the deformation field in a flexbeam, the polynomial shape function of equation (9) is truncated to obtain the approximate representation of the true axial, bending and torsional displacements.

Linear and cubic shape functions are used to express the displacements of the beam in terms of the α generalized coordinates. For axial deformations due to axial forces, the following linear shape function is employed:

$$u_a = \alpha_1 + \alpha_2 x \tag{32}$$

This shape function satisfies rigid body motion, constant strain states conditions and the compatibility conditions.

For deformations due to bending about the y and z axes, the following cubic shape functions are used:

$$v_b = \alpha_3 + \alpha_4 x + \alpha_5 x^2 + \alpha_6 x^3 \tag{33}$$

$$w_b = \alpha_7 + \alpha_8 x + \alpha_9 x^2 + \alpha_{10} x^3 \tag{34}$$

where v_b is the displacement due to bending about the z axis and w_b is the bending displacement about the y axis. These shape functions are also compatible and complete. The compatibility conditions at the ends of the element are met on displacements as well as the slopes.

For deformations due to torsion, the following linear shape function is used

$$\theta = \alpha_{11} + \alpha_{12}x \tag{35}$$

With the above shape functions, and the general expressions for the element matrices given by equations (26) to (28) and (31), the element matrices can be easily obtained via a symbolic manipulation program such as SMP.

Having the element matrices constructed, the assembly and the solution of the equations of motion are a routine matter.

Simplification of Equations of Motion

Element matrices given by equations (26) to (30) can be further simplified for the flexbeam application. We start with equation (28), the second integral, which represents the softening effect of the frame rotation on the element stiffness matrix. This term is usually small compared to the first integral if the rotor angular velocity is not close to one of the structural natural frequencies. For flexbeam design, it is small if the rotor angular velocity is not close to the first lead-lag frequency of the nonrotating flexbeam. Neglecting this term will make the model stiffer than the real flexbeam, and hence will make the prediction of stresses more conservative.

The second set of terms which can be neglected in the flexbeam design is the first three integrals in equation (30). These integrals represent the effect of large rotations on the equilibrium equations of the flexbeam. For angles smaller than 15° this term is much smaller than the structural stiffness $K^{\alpha}_{u_l}$ and the centrifugal stiffness B_σ. In a flexbeam design this term can also be neglected, resulting in more a conservative design.

Finally, the calculation of the centrifugal stiffness matrix, B_σ, can be simplified by noting that most of the CF force is caused by the weight of the blade and the pitchcase. Since the weight of the flexbeam is negligible compared to the weight of the blade and the pitchcase, we can assume that the CF force remains constant throughout the length of the flexbeam. The magnitude of this force can then be calculated separately and used as input to the program. This will eliminate the extra calculations otherwise needed to compute this force and hence results in saving computational time.

Equivalent Flexbeam Composite Properties

The composite properties of the flexbeam in the principal material directions can be obtained using the Halpin-Tsai equations of Ref.(2) as follows:

$$E_1 = \varsigma E_f + (1 - \varsigma) E_m \tag{36}$$

$$E_2 = \frac{(1 + 2\varsigma)}{(1 - \varsigma)} E_m \tag{37}$$

$$G_{12} = \frac{G_m [G_f + G_m + (G_f - G_m)\varsigma]}{G_f + G_m - (G_f - G_m)\varsigma} \tag{38}$$

$$\nu_{12} = \varsigma \nu_f + \nu_m (1 - \varsigma) \tag{39}$$

where

E_1 = composite Young's modulus in fiber direction

E_2 = composite Young's modulus pependicular to the fiber direction

G_{12} = composite shear modulus

ν_{12} = composite Poisson's ratio

E_f , E_m = Young's moduli of fiber and matrix, respectively

G_f , G_m = shear moduli of fiber and matrix, respectively

ν_f , ν_m = Poissons's ratio of fiber and matrix, respectively

ς = fiber volume fraction

Rigid Constraint Element

For bearingless rotor flexbeam design, a pitchcase model is required. One might attempt to use a stiff beam element for the pitchcase model; however, a stiff beam will result in an ill-conditioned stiffness matrix. Since a kinematic constraint involves a relationship between degrees of freedom, the correct approach is that of employing a multipoint constraint.

For large angular motion constraints between the degrees of freedom of an element, ideally a nonlinear constraint relationship is required. However, in flexbeam design, the angular rotations of flexbeam and pitchcase are small, and hence a linear constraint is sufficient.

To derive the rigid constraint element which will be used to represent the pitchcase, consider two node points A and B, which are connected by a rigid link. The rotational degrees of freedom of nodes A and B are θ_A and θ_B, respectively. Similarly, the displacement degrees of freedom are u_A and u_B. Assuming a rigid member between the two nodes, the displacements and rotations of node B can then be expressed in terms of the displacements and rotations of node A as

$$u_B = u_A + \theta_A \times r^{BA} \tag{40}$$

and

$$\theta_A = \theta_B \tag{41}$$

where r^{BA} is a vector from node A to node B the magnitude of which is the length of the rigid member. Writing the vector cross product in matrix form, we obtain

$$\begin{bmatrix} u_1 \\ u_2 \\ u_3 \\ \theta_1 \\ \theta_2 \\ \theta_3 \end{bmatrix}_B = \begin{bmatrix} 1 & 0 & 0 & 0 & L_z & L_y \\ 0 & 1 & 0 & -L_z & 0 & L_x \\ 0 & 0 & 1 & L_y & -L_x & 0 \\ 0 & 0 & 0 & 1 & 0 & 0 \\ 0 & 0 & 0 & 0 & 1 & 0 \\ 0 & 0 & 0 & 0 & 0 & 1 \end{bmatrix} \begin{bmatrix} u_1 \\ u_2 \\ u_3 \\ \theta_1 \\ \theta_2 \\ \theta_3 \end{bmatrix}_A \tag{42}$$

This, then, is the constraint equation relating the degrees of freedom of the outboard end of the flexbeam to the degrees of freedom of the snubber/damper element.

HUBFLEX Mathematical Model

Using the mathematical formulations presented earlier, a finite element computer program called HUBFLEX was developed. This computer program is tailored specifically for the analysis of flexbeams with rectangular cross sections.

HUBFLEX is a finite element analysis model for a cantilevered beam under centrifugal force. The model permits rapid calculation of spanwise load and stress distributions for a specific geometry flexbeam with specified material properties, centrifugal force, and modal deflections. The analysis has been validated against two- and three-dimensional NASTRAN models of equivalent beams, and has shown excellent correlation. Spanwise stress distributions can be calculated with HUBFLEX in less than 10 seconds CPU time on a Digital Equipment Corporation VAX 11/785. Substantial economies in the study of new designs are thus realized.

Analytically, HUBFLEX treats the flexbeam as fixed at the inboard end of the rotor mast. At the outboard end, radial tension, bending moments, shears, and torque are applied. The beam is a statically indeterminate structure in that the elastic/cross sectional properties influence the load distribution. When any section of the beam is modified, a complete iteration is required to determine the new load and stress distribution along the beam.

The HUBFLEX model utilizes the stiffness matrix method presented earlier to solve for flexbeam load distributions. Tension beam effects are modeled using centrifugal stiffening terms in each element, B_σ in equation (28). The effect of the pitchcase redundant load path is modeled by a rigid element, equation (42), attached to the flexbeam at the outboard end and attached to the flexbeam at the inboard end by a snubber/damper of given stiffnesses in the flapwise and chordwise directions. In the chordwise direction, the spring stiffness corresponds to the stiffness of the damper pads. In flap, the spring rate is equal to the stiffness of the snubber corrected for the pitchcase flapwise flexibility. The pitchcase is rigidly attached to the flexbeam at its outboard end. Inputs to the program include section element definition, flexbeam geometry, material properties, applied loads, and the desired deflections/rotations at the blade attachment point. The input forces and moments represent those applied to the flexbeam by the blade spanwise moment and shear distributions. The shear to moment ratios at the blade attachment have a powerful influence on the flexbeam deflected shape and are determined separately in an iterative procedure. They are continually updated as the configuration evolves. The spanwise load and stress distribution results include the effect of combined loadings associated with the relative phasing of the flap, chord, and torsion motions. As with the shear to moment ratios, the phasing has a powerful influence on the final results especially for the critical shear loads due to combined normal bending and feathering. The phasing relationships were defined using an aeroelastic analysis (DART) and were verified by the HARP flight test results.

HUBFLEX/ADS Computer Program

The HUBFLEX finite element model was initially used to study flexbeam geometries that were established by engineering judgment. Because of the indeterminate nature of the problem and the millions of possible geometry variations which could be developed, engineering judgment was deemed inadequate to quickly define an optimum (lowest stresses) configuration. In addition, an optimum configuration for one specific flight condition, such as cruise flight, was significantly different from a configuration which would produce minimum stresses in a maneuver condition. To address this problem an optimization routine called ADS (Automated Design Synthesis), Ref. (3), was added to the HUBFLEX analysis program. The routine permitted holding certain parameters of the design fixed or within specified bounds while freeing other variables to achieve a minimum stress distribution along the length of the beam. A further enhancement was added by providing for the weighted optimization of several flight conditions simultaneously. A block diagram of the optimization procedure is provided in Figure (2).

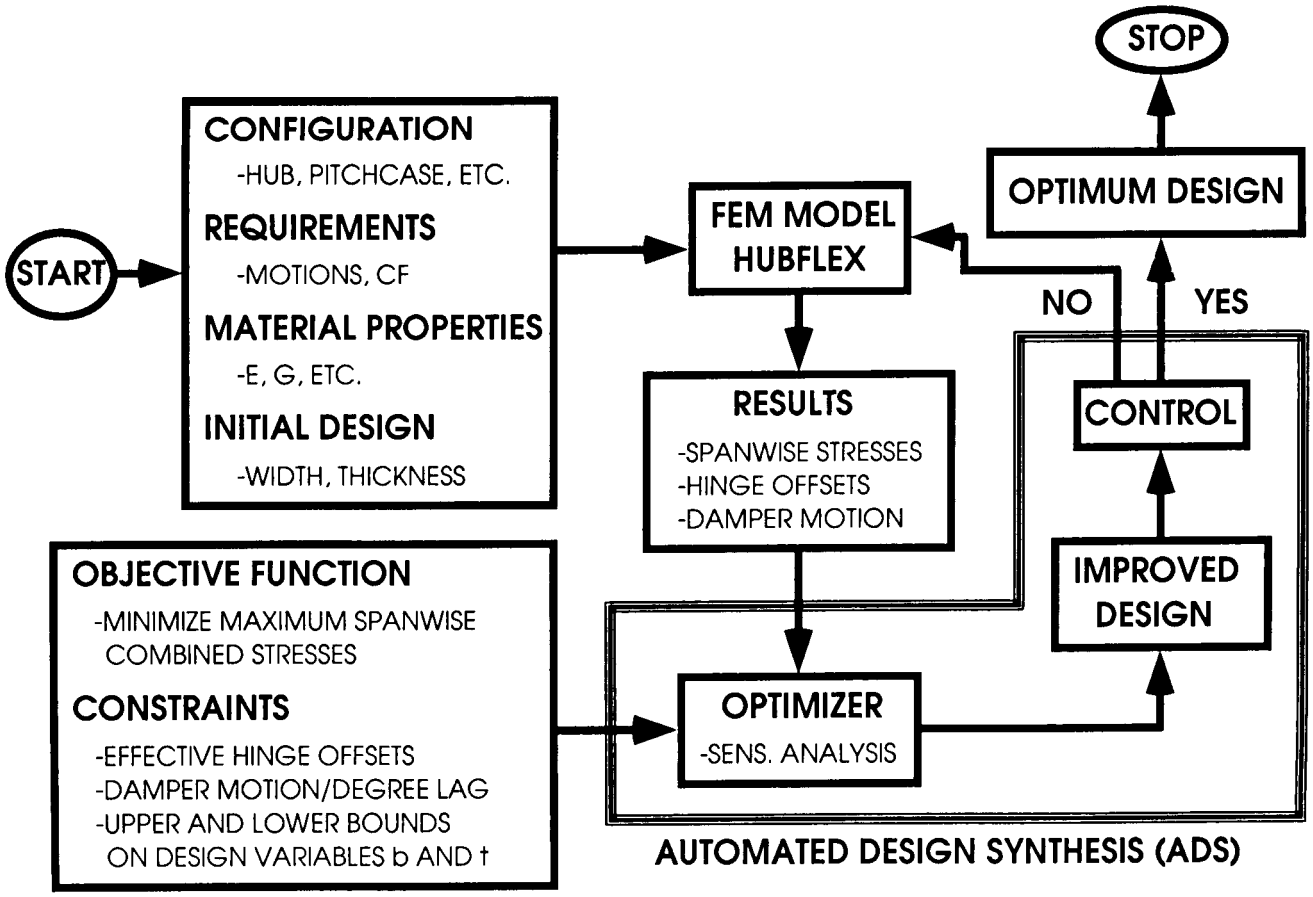

Figure (2)

In practice, the optimization program was used to minimize the maximum stresses (normal and shear) caused by maximum maneuver and endurance motions. Design variables were the dimensions of the beam element, with upper and lower bounds established for manufacturing feasibility. The required damper motion per degree lag motion was selected as a constraint in the optimization process.

The results of this work led to the highly tailored design configurations established for three different flexbeams for three different helicopters. These are, ACH (Advanced Composite Hub), advanced HARP and most recently, the MDX*flexbeam. The advanced HARP flexbeam was designed in less than a week (the old HARP flexbeam took more than 6 months), while it took only half a day to design a flexbeam for the MDX main rotor. The reduction of design time from one week for advanced HARP to half a day for the MDX flexbeam was purely due to postprocessing of the optimization results. The postprocessing of the advanced HARP flexbeam results was carried out by hand and relied upon engineering judgment, while the postproccessing of the MDX flexbeam optimization results was done by computer and hence human factors and consequently excessive time was removed completely from the optimization process.

In general, it was found that the endurance level flight condition dictated the geometry of the outer portion of the beam where high cycle shear stresses were most critical. The low-cycle high g maneuver condition dictated the beam geometry of the inboard end due to high normal stresses.

Among the three optimized flexbeams, the advanced HARP is the only one which has been fabricated and successfully tested in fatigue as well as in the Duits Nederlandse Windtunnel (DNW).

Optimization Results

The finite element optimization program HUBFLEX/ ADS was used to optimize the advanced HARP flexbeam. The composite material selected for the advanced beam was S2-Glass fiber and the matrix was Epoxy. The maximum combined normal and/or shear stresses for the one hour flight condition as well as endurance were selected as the objective function. To achieve at least 3% critical damping, a damper motion of 0.1 inch per degree lag was required. Therefore a lower constraint was put on the damper motion. In addition to this active constraint, to insure the continuity of fibers, a set of constraints was put on the beam cross sectional area variation over the length of the beam such that the area was required to either decrease or remain constant, but was not allowed to increase from inboard to outboard. In addition to these constraints, lower and upper constraints were imposed on the dimensions of the beam element, based on manufacturing requirements.

---

* McDonnell Douglas (X)

The HUBFLEX/ADS computer program was used to optimize the advanced beam based on the above optimization statement. A comparison between the initial design and the optimum design for the advanced beam is shown in Table(1). As can be seen in this table, it took more than 6 months to design the old flexbeam with unacceptable stresses. However with the HUBFLEX/ADS program, an acceptable configuration was obtained in a week, with acceptable stresses. The damper motion per degree lag, the hinge offsets in flap and lag directions, and the corresponding first frequencies for both the old and the advanced beams are acceptable as shown in the table. The alternating angles for which the old and the advanced beams were designed are also shown in the table.

A three-dimensional view of the advanced beam is shown in Figure (3). As seen in the figure, the variations of width and thickness are such that the geometric area of the beam section is always decreasing or is constant. This particular requirement insures the continuity of the fibers.

Table(1)

PARAMETER	"OLD" HARP	NEW HARP
Time to design configuration	6 mo.	1 wk.
Normalized max combined normal stresses	1.70	1.04
Normalized max combined shear stresses	0.96	1.03
Damper motion per deg. lag	0.18	0.16
$\frac{e_\mu}{R} \times 100$	5.3	4.2
$\frac{e_\zeta}{R} \times 100$	24.8	15.6
$\frac{\omega_\mu}{\Omega}$	1.06	1.04
$\frac{\omega_\zeta}{\Omega}$	0.61	0.50
β	6.8	6.8
ς	2.0	2.0
θ	11.5	11.5

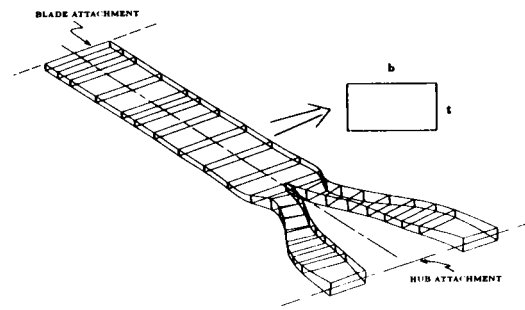

Figure (3)

HUBFLEX/NASTRAN Comparison

In the development stage, the HUBFLEX program was validated against 2-dimensional and 3-dimensional equivalent beam NASTRAN models and showed excellent correlation.

For the advanced HARP program, an additional level of verification was obtained by creating a 3-dimensional nonlinear anisotropic solid element NASTRAN model of the detailed flexbeam structure. The model was constructed using 3048 8-noded (octahedron) and 8 6-noded (hexahedron) solid elements incorporating over 12,000 degrees of freedom, Figure (4). The snubber damper centering bearing was rigidly attached to the flexbeam using constraint equations. The chordwise and flapwise damper stiffnesses were represented by elastic springs and attached to a rigid element pitchcase. The inboard end of the flexbeam was rigidly constrained. The outboard blade attachment location was multipoint constrained to allow loads and the pitchcase attachment to be applied at a single centerline grid point.

The detailed nonlinear model was run for flap, lead-lag and feathering one hour flight motions using MSC/NASTRAN's geometric nonlinear solution 64 (whose algorithm is an extension of the differential stiffness approach, Ref (4)). The CF loading was applied in the linear elastic step and then combined with the corresponding flap, lead-lag and feathering loading in the following differential stiffness step. The combined loading was then taken through one additional nonlinear interation for an improved solution. Computation time for each run amounted to 8 hours of CPU time running on a VAX 11/785.

The primary loading condition of interest was lead-lag where the HUBFLEX program approximates the chordwise stiffness of the split leg/shear web section of the flexbeam by an equivalent 'I' beam moment of inertia.

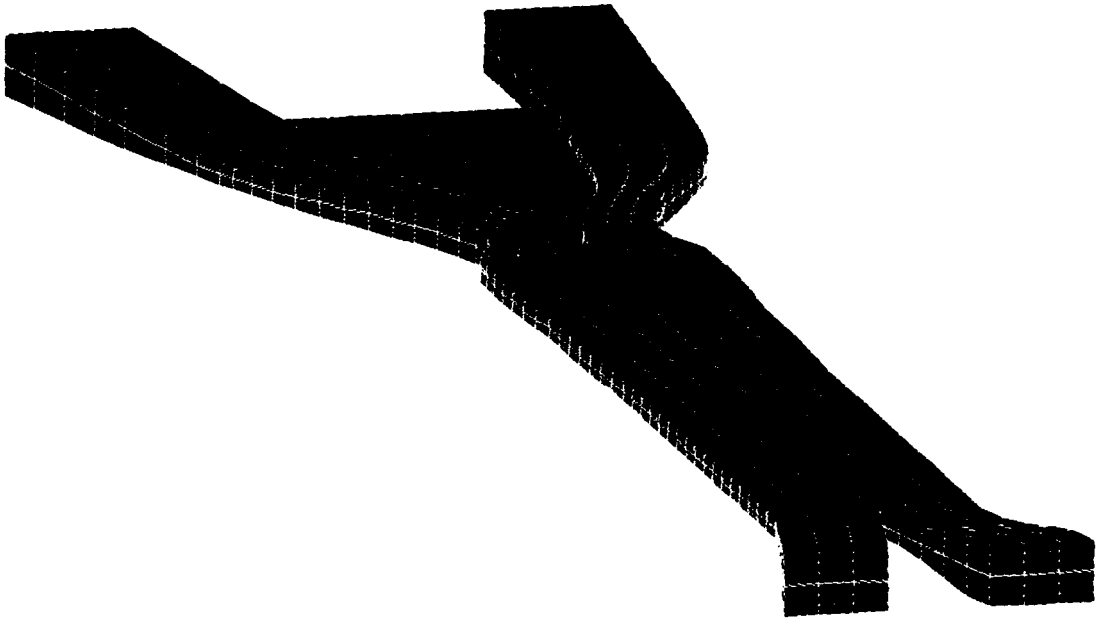

Figure (4)

ORIGINAL PAGE
BLACK AND WHITE PHOTOGRAPH

In order to compare with the HUBFLEX output of spanwise displacements, a set of grid points on the centerline of the flexbeam was selected to represent the overall deformation. For the comparison of spanwise normal stress distributions, element stress peak values obtained within the corresponding cross section location were used.

Correlation of chordwise loading indicated that the HUBFLEX chordwise stiffness approximation produced a stiffer beam resulting in conservative peak stress values that were approximately 10 percent higher than those of the detailed solid element model. A comparison of the chordwise displacement and spanwise stress distribution is provided in Figures (5) and (6).

For the trivial flapwise and feathering loading cases, correlation was excellent as expected. Peak stress values were typically 3 to 5 percent higher for the HUBFLEX model. Figures (7) and (8) demonstrate this correlation for the flapwise loading case.

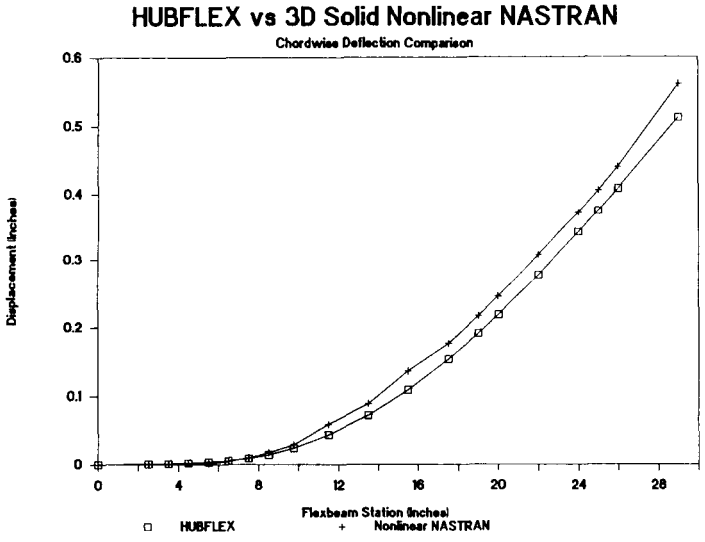

Figure (5)

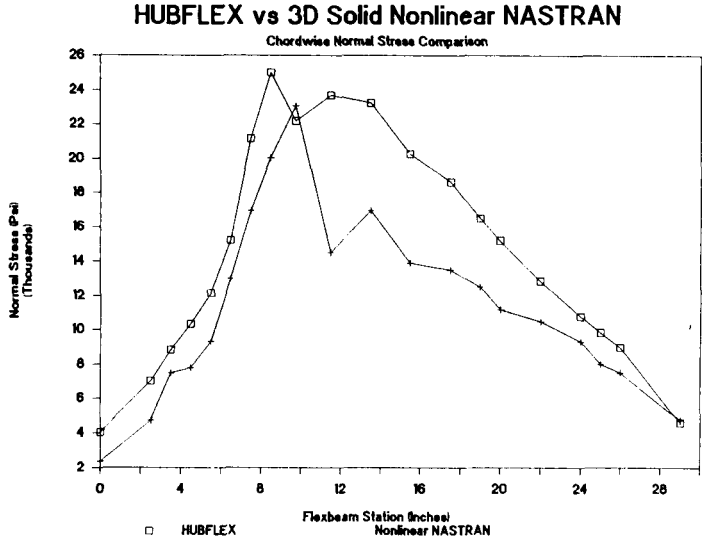

Figure (6)

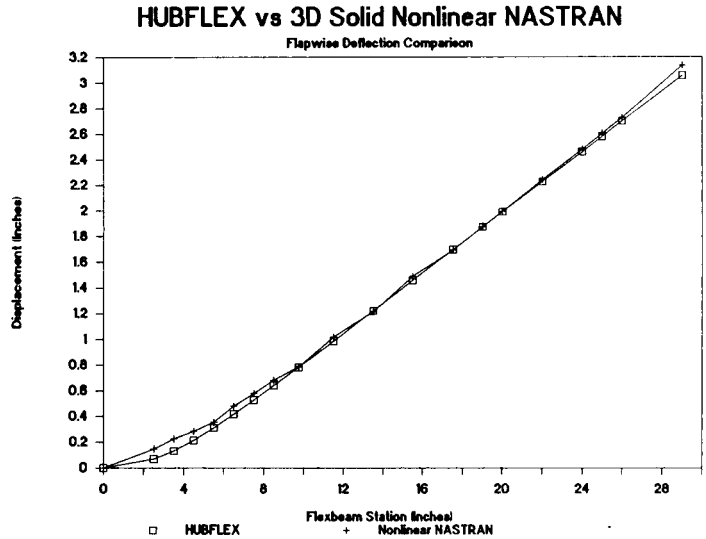

Figure (7)

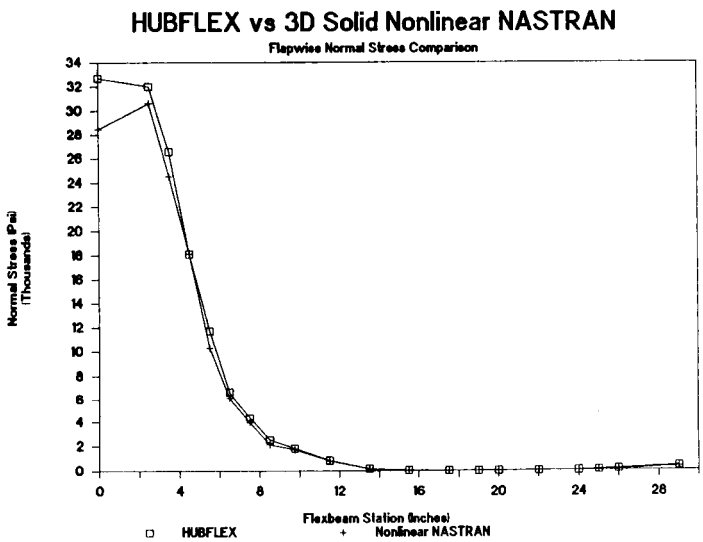

Figure (8)

Conclusions

1. Pitchcase and snubber damper representations are required in the flexbeam model for proper sizing resulting from dynamic requirements.
2. Optimization is necessary for flexbeam design. It reduces the design iteration time and results in an improved design.
3. Inclusion of multiple flight conditions and their corresponding fatigue allowables is necessary for the optimization procedure.
4. A simplified beam model is adequate for flexbeam sizing. The simplified model gives excellent accuracy (compared to a detailed 3D nonlinear NASTRAN analysis) with a significant reduction in computational time.
5. HUBFLEX's rapid computation capability enables design parameters to be easily modified and implemented.

References

1. Zienkiewicz, O.C., "*The Finite Element Method*", 3rd Edition, McGraw Hill Book Co., New York, 1982.
2. Jones, R.M., "*Mechanics of Composite Materials*", McGraw Hill Book Co., New York, 1973.
3. Vanderplaats, G.N., "*ADS - A Fortran Program for Automated Design Synthesis*", Version 1.00 , NASA Contract Report 172460, Langley Research Center, Hampton, Virginia, 1984.
4. MSC/NASTRAN Application Manual, Macneal- Schwendler Corporation, March 1981.